



5.1 Optics Specifications

Jared R. Males

1 Introduction

This document describes the specifications for the optical components of MagAO-X, including surface quality and coatings. We include our knowledge of the existing telescope optics, and the expected performance of the wavefront control systems.

In this analysis we assume polished optics follow a von Kàrmàn-like PSD of the following form

$$\mathcal{P}(\vec{k}) = \frac{\beta}{\left((1/L_0)^2 + |\vec{k}|^2\right)^{\alpha/2}} e^{-(|\vec{k}|l_0)^2} + \beta_{sr}. \quad (1)$$

where \vec{k} is the spatial frequency, β is a normalization constant, α is the PSD index, L_0 is an outer scale (low frequency flattening), and l_0 is the inner scale (high frequency roll-off), and β_{sr} is the surface roughness (the floor reached at high spatial frequency). See Appendix A for a detailed justification of this model using representative PSDs, as well as the methods we use to project the PSDs of various optics onto the primary mirror.

The wavefront error (WFE) analysis presented here does not take into account diffraction, rather our goal is to quickly compare trades in the various possible specifications. See the Fresnel model of the system for a diffraction-based analysis.

2 Requirements

This analysis is concerned primarily with the static and non-common path (NCP) wavefront errors (WFEs). These sources of WFE affect the Strehl ratio and the contrast. The requirements on the optical surface quality are derived from the high-level science requirements, in conjunction with the performance simulations and error budget. They are

- Requirement: Static/NCP WFE < 45 nm rms. At H α this multiplies Strehl ratio by 0.83. This specification ensures that the bright star Strehl ratio requirement of 70% can be met.
- Goal: Static/NCP WFE < 35 nm rms. Strehl ratio (S) due to static/NCP impacts exposure time as $t \propto S^3$. Hence we should seek maximum possible performance.
- Requirement: Static/NCP WFE contribution to contrast should be $< 1 \times 10^{-3}$ from 0 to 24 λ/D . This is after the effects of low-order WFS (LOWFS) and/or focal-plane WFS (FPWFS) are taken into account.

All of these requirements are derived for the science channel. The WFS channel requirement is simply that it should not be worse, as it has fewer optics.



3 The Clay Telescope

MagAO-X is designed for the 6.5 m Magellan Clay telescope. Here we present analysis of the primary mirror (M1), the f/11 fixed secondary (M2), and the tertiary mirror (M3).

3.1 M1: The Magellan Clay primary mirror was cast and polished at the Steward Observatory Mirror Lab (SOML). The post-polishing test data were analyzed (see Appendix B). The surface map is shown in Figure 1. The surface height has 12.52 nm rms across all spatial frequencies sampled by the map. Figure 2 shows the surface map with 29% central obscuration (defined by the secondary baffle) and with the outer edge masked by 4.4% to mask the jagged edge. This also has a 12.52 nm rms, only negligibly reduced from the unmasked map.

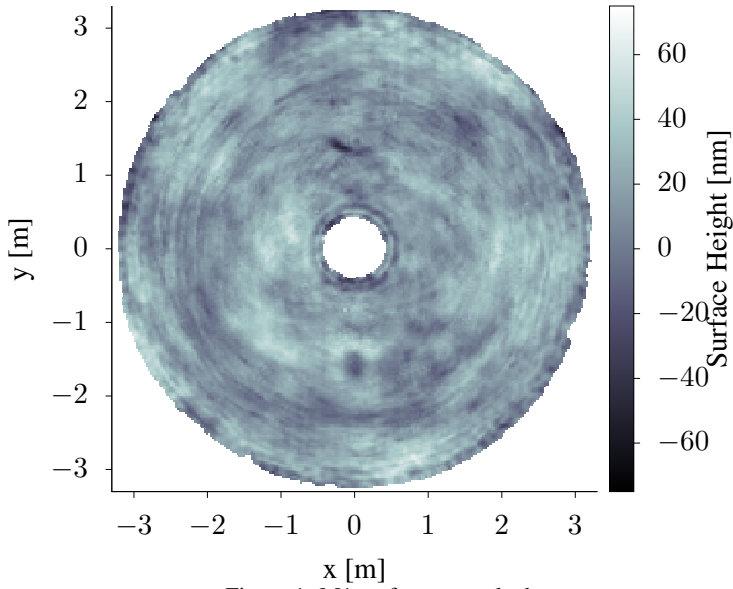


Figure 1: M1 surface unmasked

Using the un-masked surface map we calculated the 2D PSD of the masked surface. An annular Hann window was applied before the FFT, and the resultant PSD was renormalized to have total variance corresponding to 12.52 nm rms. Figure 3 shows the median radial profile of the PSD. The best fit (in log space) has slope $\alpha = -2.8$, a very steep power law.

See Appendix B for additional analysis of the M1 surface.

3.2 Pupil Definition : The Magellan Clay telescope secondary mirror baffle forms a 29% central obscuration. The secondary is supported by 4 supports, called vane ends at Magellan, a.k.a. spiders. Using a 3D model of the telescope (provided by Charlie Hull), we found the spiders to be offset by 0.34 m from the center, and running at 45°. The vane end struts are nominally 0.75" wide. On two of them the MagAO cable-trays, used to route power and cooling to the ASM, increase the width to 1.5". These are thin relative to other observatories (e.g. Subaru is reported to have 20 cm wide spiders).

For analysis and simulations pupil masks were made informed by the above specifications. Two masks were

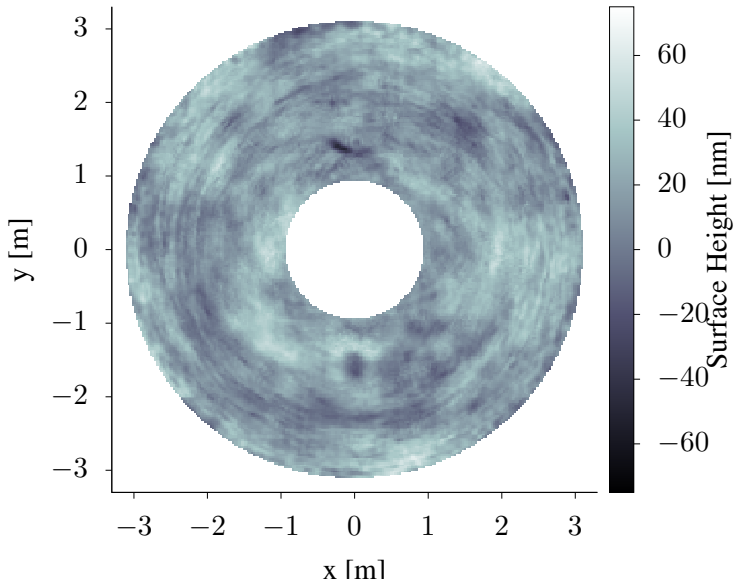


Figure 2: M1 surface masked with a 95.6% outer radius and 29% central obscuration.

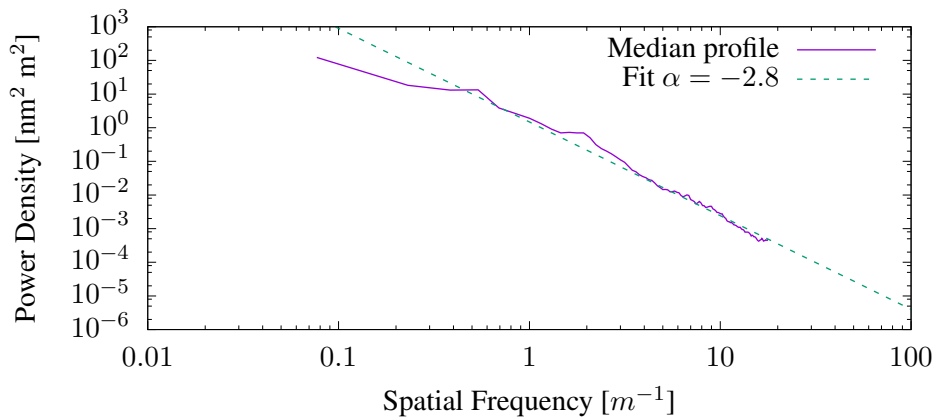


Figure 3: Median radial profile of the PSD of M1 surface.

made:

1. Input Pupil. This is 6.5m wide, with a 29% central obscuration. Grayscale is used for the spiders to account for their width relative to the pixel scale in the mask (calculated by re-binning larger arrays). This is used as the input for end-to-end simulations, etc.



2. Coronagraph Pupil. This mask is intended for use in the coronagraph arm. The goal of this mask is to oversize the various features (undersize the pupil overall) to ensure that coronagraph designs are feasible and alignment tolerances can be met. The outer diameter is undersized to 95.6% (6.21 m projected) to mask out the rough outer edge identified above. The central obscuration is oversized to 31% of the undersized diameter, which corresponds to 1/2 an actuator projected onto the high-order (MEMS) DM. The spider masks are binary and oversize to 68 mm. For scale, this corresponds to a 0.3° tolerance in the pupil rotation alignment.

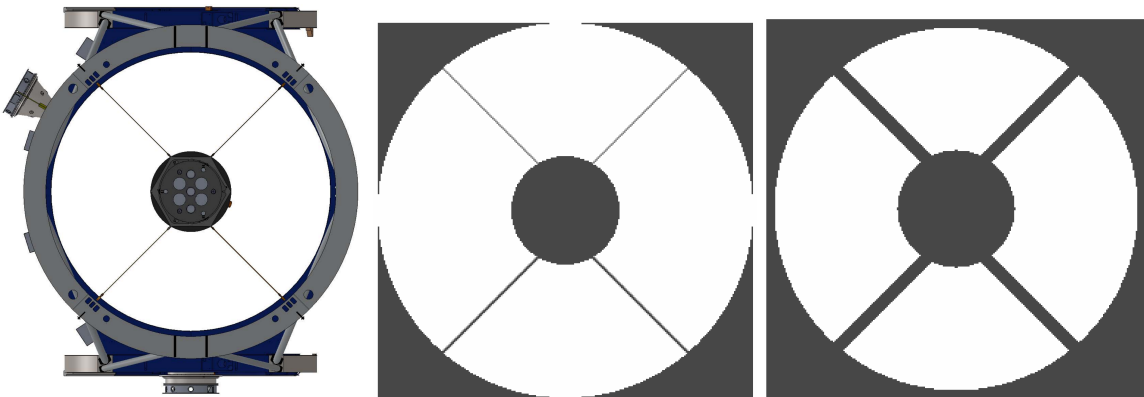


Figure 4: Defining the MagAO-X pupil. Left: solid model of the telescope showing. Middle: input pupil mask. Right: coronagraph channel mask.

3.3 M2: A post-fabrication measurement of the surface structure function of the Clay f/11 static secondary is shown in Figure 5. We fit this to a power law with index $\alpha - 2$, where α is the index of the spatial PSD as in Equation (1) (Noll, 1976). The measurements indicate that the surface of M2 has 12.7 nm rms.

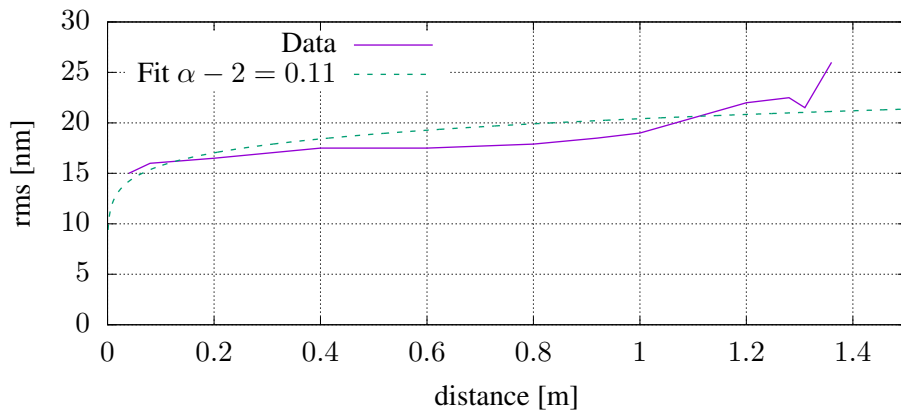


Figure 5: Measured structure function of the static f/11 (M2) and our power-law fit.



3.4 M3: From the manufacturer's test report for the (now re-coated) tertiary mirror, we have the surface map shown in Figure 6. We analyzed this map using the same procedure as for M1, and found the PSD shown in Figure 7. M3 has a reported surface finish of 13.8 nm rms, with a best fit PSD having $\alpha = 3.28$.

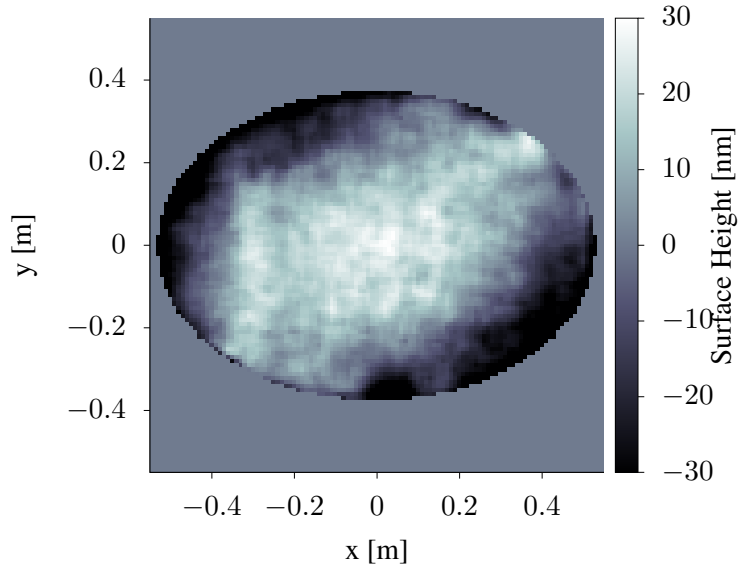


Figure 6: M3 surface.

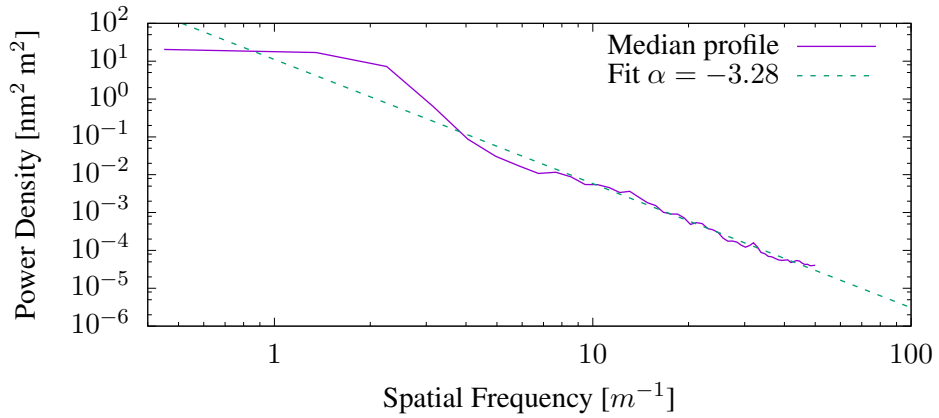


Figure 7: M3 PSD from a circular aperture.



4 Deformable Mirrors

Here we describe the specifications of the deformable mirrors we will use for wavefront correction. For this analysis, in all cases we assume that the flat surface quality is perfect within the device's spatial control bandwidth, so the given surface quality is for the remaining higher spatial frequencies. We assume a PSD with $\alpha = 2$ for these surfaces.

4.1 High Order DM: The high order DM, or tweeter, is a Boston Micromachines Corp. MEMS 2k. This is a 2048 actuator device, with 50 actuators across a circular aperture. BMC has guaranteed a 100% yield device within the clear aperture described by pupil (allowing for a limited number of bad actuators under a spider). The main optical characteristics are summarized in Table 1.

The nominal device we have specified is a $1.5 \mu\text{m}$ P-V stroke DM. BMC has begun working to determine if they have a $3.5 \mu\text{m}$ stroke 2k DM already fabricated which meets our yield needs. If they do, we have the option of taking this device. In this case, all other specifications (other than stroke) remain the same. Actuator stroke requirements are addressed in the simulation section.

Table 1: Boston Micromachines 2k Specifications.

	Total Act.	Linear Act.	Pitch [mm]	CA mm	Flat surface Max Spec	[nm rms] Typical
Value:	2048	50	0.4	19.7	20	13

4.2 Low Order DM: We plan to use the Alpao DM97-15 for our low order DMs. We have designed in two of these. The first serves as the woofer to minimize the stroke requirements on the BMC 2k tweeter. The second will be used in the science channel (after the HOWFS beamsplitter), under control by the LOWFS. This allows for correction of non-common path errors sensed by the LOWFS.

The main optical characteristics are summarized in Table 2.

Table 2: Alpao DM97-15 Specifications.

	Total Act.	Linear Act.	Pitch [mm]	CA mm	Flat surface Max Spec	[nm rms] Typical
Value:	97	11	1.5	13.5	7	4

5 WFE of the MagAO-X Design

Now we proceed to analyze the specifications needed in the remaining optics of the system.

5.1 Available Optics: Quotations from two vendors have been obtained for off-axis parabolas. Their parameters are summarized in Table 3. We have not yet obtained detailed quotes for flats, but flats of high quality are readily available from various vendors so we use specifications typical for such optics.

5.2 Optical Design: The detailed opto-mechanical design is presented in section 2.1. Tables 4 and 5 list the optical surfaces in the MagAO-X design which are considered here.



MagAO-X Preliminary Design

5.1 Optics Specifications

Doc #: MagAOX-001
 Date: 2017-04-19
 Status: Rev. 0.0
 Page: 7 of 18

Table 3: Possible optic specifications

Type	Manufacturer & Description	D_{CA} [mm]	Specified				PSD		Notes
			λ_t [nm]	PV [nm rms]	σ [nm rms]	d [mm]	α	β^4 [nm ²]	
OAP	Vend. 1 Standard	40.0 ¹	—	—	63.3	5.0	1.55	94.98	Spec'd in refl. WFE
OAP	Vend. 1 Precision	40.0 ¹	—	—	31.7	0.5	1.55	5.23	Spec'd in refl. WFE
OAP	Vend. 1 High Prec.	40.0 ¹	—	—	12.7	0.5	1.55	0.84	Spec'd in refl. WFE
OAP	Vend. 2 $\lambda/8$	41.1 ²	633	79.1	—	—	1.55	85.46	Spec'd in surf. error
OAP	Vend. 2 $\lambda/20$	43.4 ²	633	31.7	—	—	1.55	13.97	Spec'd in surf. error
FLAT ³	$\lambda/20$	50.8	—	31.7	—	—	2.0	63.63	Spec'd in surf. error
FLAT ³	$\lambda/50$	50.8	—	12.7	—	—	2.0	10.18	Spec'd in surf. error
FLAT ³	$\lambda/100$	50.8	—	6.33	—	—	2.0	2.55	Spec'd in surf. error
FLAT ³	$\lambda/200$	50.8	—	3.16	—	—	2.0	2.55	Spec'd in surf. error

¹ CA for Vendor 1 could be 35-40 mm for the 50 mm OAPs.

² CA varies in Vendor 2 quote.

³ Quotes for flats not yet obtained.

⁴ β specified for reflected wavefront error.

Table 4: MagAO-X Optical Surfaces – Common Path.

No.	Type	Name	D_{beam}	θ_i	Coating	Notes
Common Path						
1	Primary	M-1	6.5	0.0	Al	
2	F/11	M-2	1.36	0.0	Al	
3	Tertiary	M-3	1.1	45.0	Custom	
4	Flat	F-1	2.9	45.0	P-Ag	
5	Flat	F-2	2.9	45.0	P-Ag	
6	OAP	O-0	13.7	32.5	P-Ag	
7	Flat	K-1	13.4	60.0	P-Ag	
8	Flat	K-2	13.2	30.0	P-Ag	
9	Flat	K-3	13.5	60.0	P-Ag	
10	Woofer	LODM	13.5	15.0	P-Ag	Alpao DM-97
11	OAP	O-1	14.1	26.5	P-Ag	
12	Flat	F-3	13.0	17.5	P-Ag	
13	OAP	O-2	20.41	10.0	P-Ag	
14	Tweeter	HODM	19.41	8.4	UnP-Au	BMC 2K
15	OAP	O-3	22.97	7.5	P-Ag	
16	Flat	F-4	20.0	45.0	P-Ag	Down to lower level
17	Flat	F-5	6.4	45.0	P-Ag	From upper level
18	OAP	O-4	12.56	7.5	P-Ag	
20	Flat	F-6	10.8	48.5	P-Ag	Possible DM
21	ADC	ADC-1			AR	
22	ADC	ADC-2			AR	
23	ADC	ADC-3			AR	
24	ADC	ADC-4			AR	



MagAO-X Preliminary Design

5.1 Optics Specifications

Doc #: MagAOX-001
Date: 2017-04-19
Status: Rev. 0.0
Page: 8 of 18

Table 5: MagAO-X Optical Surfaces – Non-Common Path.

WFS						
W-25	Beamsplitter	BS-1-T	—			Transmission to WFS
W-26	Flat	TTM	9.0	42.0	P-Ag	PYWFS Modulator
W-27	OAP	O-5	13.31	7.5	P-Ag	Same optic as C-28, different footprint
W-28	Flat	F7	10.7	30.0	P-Ag	
W-29	Pyramid	PYR-1	—			
W-30	Pyramid	PYR-2	—			
W-31	Pyramid	PYR-3	—			
W-32	Pyramid	PYR-4	—			
W-33	Zoom lens	PZL-1	—		AR	For pupil magnification and positioning.
W-34	Zoom lens	PZL-2	—		—	For pupil magnification and positioning.
W-35	Zoom lens	PZL-3	—		—	For pupil magnification and positioning.
W-36	Zoom lens	PZL-4	—		AR	For pupil magnification and positioning.
Coronagraph						
C-25	Beamsplitter	BS-1-R	10.3	42.0	—	Reflection
C-26	Flat	F-8	9.3	42.0	P-Ag	
C-27	Flat	F-9	10.3	42.0	P-Ag	
C-28	OAP	O-5	13.31	7.5	P-Ag	Same optic as W-27, different footprint
C-29	Fold	F-10	7.2	7.5	P-Ag	
C-30	FPM	FPM	—			
C-31	OAP	O-6	13.3	7.5	P-Ag	
Coronagraph focal plane						
C-32	Lyot Stop	LS-T	—			
C-33	Fold	F-11	10.2	7.5	P-Ag	
C-34	OAP	O-7	13.3	7.5	P-Ag	
C-35	Fold	F-12	—		P-Ag	
C-36	SDI	—	—			multiple surfaces
Coronagraph Lyot plane						
L-32	Lyot Stop (flat)	LS-R	9.0			
L-33	Lens	L-L-1	9.0		AR	



5.3 Spec Comparison: PSDs for each of the optics were constructed according to the specifications in Table 3. These were added, grouped as common path (CP), non-common path (NCP) in the WFS and science channels. The CP optics had all power up to $1/(2d_{ho})$ removed, assuming that the WFS and LODM and HODM remove these aberrations. The NCP optics had all power removed up to $1/(2d_{lo})$, assuming that the LOWFS and LOWFS-DM remove this power.

The resultant rms WFE for each grouping are given in the tables below, for different combinations of the OAP and flat specifications. Here we assume $D/d_{lo} = 11$, that is ~ 97 modes are corrected by the LLOWFS using the LLOWFS-DM.

Table 6: Uncorrectable Common Path WFE (nm rms waveform)

OAPS	Flats:	No BMC				BMC 20 nm rms flat				BMC 13 nm rms flat			
		$\lambda/20$	$\lambda/50$	$\lambda/100$	$\lambda/200$	$\lambda/20$	$\lambda/50$	$\lambda/100$	$\lambda/200$	$\lambda/20$	$\lambda/50$	$\lambda/100$	$\lambda/200$
Vend. 1 Standard		229.1	218.7	217.1	216.7	231.2	220.8	219.3	218.9	230.0	219.6	218.1	217.7
Vend. 2 $\lambda/8$		219.2	208.2	206.6	206.2	221.4	210.5	208.9	208.5	220.1	209.2	207.6	207.2
Vend. 2 $\lambda/20$		113.1	90.1	86.3	85.3	117.3	95.2	91.7	90.7	114.9	92.3	88.6	87.6
Vend. 1 Precision		90.9	59.8	53.9	52.3	96.0	67.3	62.1	60.7	93.1	63.0	57.5	56.0
Vend. 1 High Prec.		79.2	39.8	30.2	27.3	85.0	50.4	43.2	41.2	81.7	44.5	36.3	33.9

Table 7: Non-Common Path WFE (nm rms waveform)

OAPS	Flats:	WFS Channel				Science Channel			
		$\lambda/20$	$\lambda/50$	$\lambda/100$	$\lambda/200$	$\lambda/20$	$\lambda/50$	$\lambda/100$	$\lambda/200$
Vend. 1 Standard		183.7	169.2	167.1	166.5	188.9	180.5	179.2	178.9
Vend. 2 $\lambda/8$		176.4	161.3	159.0	158.4	180.6	171.8	170.5	170.2
Vend. 2 $\lambda/20$		100.9	71.2	65.9	64.5	91.8	73.0	69.9	69.1
Vend. 1 Precision		86.5	48.8	40.6	38.3	72.9	47.1	42.1	40.8
Vend. 1 High Prec.		79.3	34.6	21.6	16.9	62.8	29.1	20.2	17.2

5.4 DM Stroke: To ensure that the static and NCP corrections do not saturate the DMs, we also analyzed the stroke requirement these corrections impose. These are shown in Tables 8 and 9. The BMC HOWFS has a minimum interactuator stroke of 855 nm, and the Alpa DM has a minimum interactuator stroke of 2500 nm. We conclude that DM stroke is more than sufficient to handle the static and NCP errors (dynamic stroke requirements are addressed in the simulation section).

Table 8: Stroke Used By HOWFS (nm rms).

OAPS	Flats:	Woofer				Tweeter			
		$\lambda/20$	$\lambda/50$	$\lambda/100$	$\lambda/200$	$\lambda/20$	$\lambda/50$	$\lambda/100$	$\lambda/200$
Vend. 1 Standard		177.7	154.7	151.1	150.2	185.8	171.5	169.4	168.8
Vend. 2 $\lambda/8$		172.8	149.1	145.4	144.4	178.8	163.8	161.6	161.0
Vend. 2 $\lambda/20$		127.8	93.2	87.1	85.6	108.0	80.8	76.2	75.0
Vend. 1 Precision		120.8	83.3	76.5	74.7	95.1	62.6	56.5	54.8
Vend. 1 High Prec.		117.6	78.6	71.3	69.4	88.8	52.6	45.2	43.1



MagAO-X Preliminary Design

5.1 Optics Specifications

Doc #: MagAOX-001
 Date: 2017-04-19
 Status: Rev. 0.0
 Page: 10 of 18

Table 9: Stroke Used By LOWFS (nm rms).

OAPS	Flats:	LOWFS-DM			
		$\lambda/20$	$\lambda/50$	$\lambda/100$	$\lambda/200$
Vend. 1 Standard		103.3	90.8	88.9	88.4
Vend. 2 $\lambda/8$		99.6	86.6	84.6	84.1
Vend. 2 $\lambda/20$		63.5	40.2	35.6	34.4
Vend. 1 Precision		57.2	29.3	22.6	20.6
Vend. 1 High Prec.		54.2	22.9	13.4	9.6

6 Contrast

Finally, we consider the effect of static/NCP aberrations on the contrast. The raw PSF-profile contrast at a given separation is given by the variance of the WFE in radians in the Fourier mode corresponding to that separation. Using this fact, and the PSDs calculated for the system, we present variance vs. separation profiles in Figure 8 to characterize the contrast degradation of the optical surfaces. We included the effects of LOWFS, but not FPWFS.

We compare the static/NCP variance to the dynamic variance expected from atmospheric turbulence. This is calculated using an update version of the method in Guyon (2005). This is also shown for 5th and 10th magnitude stars.

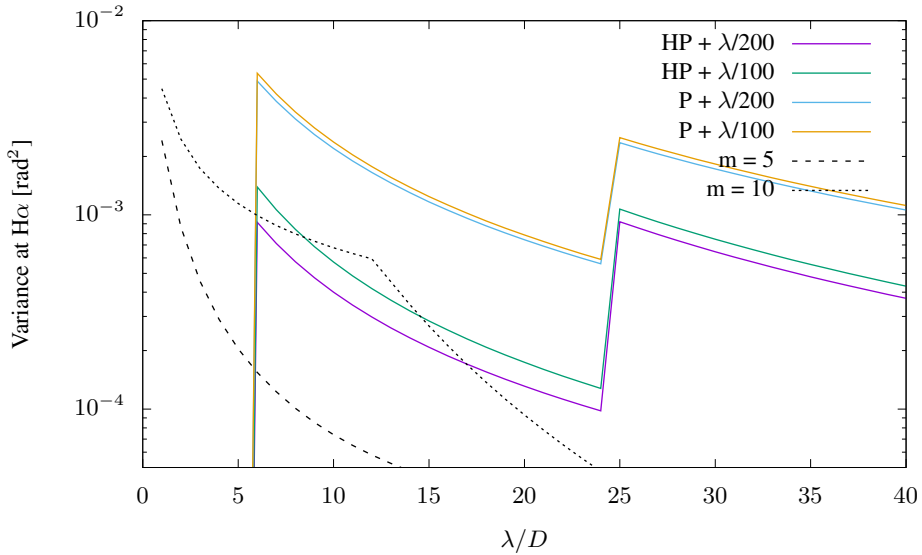


Figure 8: Variance profiles due to the optics of MagAO-X.

7 Conclusions

From this analysis we draw the following conclusions:

1. OAPs with Vendor #1's High Precision specification are required to reach the static/NCP WFE specification (45 nm rms).



2. OAPs with Vendor #1's High Precision specification are required to reach the 1×10^{-3} contrast specification.
3. The requirement on flat surface quality depends strongly on the surface quality of the BMC DM. If that is worst case 20 nm rms, then $\lambda/200$ flats are needed to meet the WFE spec. $\lambda/100$ flats are sufficient if the BMC DM is delivered with a typical 13 nm rms post-flat surface.
4. The flat specifications only weakly affect the contrast profile.
5. With the BMC DM, we are unlikely to reach the goal of 35 nm rms static/NCP WFE. This analysis shows that we can reach 38 nm rms.

We have shown that our design can meet the static/NCP WFE and contrast specifications with available optics.



A Power Spectral Densities

To understand the impact of the surface quality on both Strehl ratio and contrast, we need to know the power spectral density (PSD) of the surface. To begin with we will assume a PSD of the form

$$\mathcal{P}(\vec{k}) = \frac{\beta}{|\vec{k}|^\alpha}.$$

As we will show, this basic form is well justified in the literature. The two parameters, α and β must be determined.

A.1 PSD Normalization: The PSD can be normalized by the root-mean-square, or rms, of the departure of the optical surface from the design shape. This can be calculated as the integral of the PSD over a limited spatial-frequency band:

$$\sigma^2 = \int_{k_{min}}^{k_{max}} \frac{\beta}{|\vec{k}|^\alpha} k dk d\phi$$

This leads to the following expression for β :

$$\beta = \sigma^2 \times \begin{cases} \frac{\alpha-2}{2\pi(k_{min}^{-\alpha+2} - k_{max}^{-\alpha+2})} & \alpha \neq 2 \\ \frac{1}{2\pi \ln(\frac{k_{max}}{k_{min}})} & \alpha = 2 \end{cases} \quad (2)$$

Optical manufacturers seldom specify any of σ , k_{min} or k_{max} . In the case of one vendor, σ over a certain spatial scale, which we will refer to as l_{min} , is specified, and $k_{max} = 1/l_{min}$. Equivalently, we can specify this in terms of sampling length d , such that $l_{min} = 2d$ which gives the usual $k_{max} = 1/(2d)$.

We can safely assume that $k_{min} = 1/D_{CA}$, where D_{CA} is the diameter of the clear aperture (CA) of the optic being specified.

In cases where only a peak-to-valley (PV) figure error is specified, usually as λ_t/N where λ_t is the test wavelength, we have to make some assumptions. Depending on the low-order Zernike being considered, the ratio of PV/σ ranges from 3-6 (Evans, 2009; Schwertz, 2010). We adopt $PV/\sigma = 4$ as recommended by Schwertz (2010) as a conservative compromise which will not underestimate the WFE.

The number of Zernike modes, or equivalently the value of d , over which the PV specification is determined is almost never specified in any way. From the statements of equivalence given in Vendor 1's quote, we can infer that $D/d \approx 4-5$. We assume that the number of Zernikes (or degrees of freedom (DOF)) is $\pi/4(D/d)^2$, so this corresponds to 13–20 Zernike modes being considered in the Figure error. In Evans (2009) 36 Zernike modes are used to develop the PVr metric, corresponding to $D/d \sim 7$. A presentation by several optical engineers¹ recommends that the cutoff for Figure error be 5 – 10 cycles per aperture, or $D/d = 10 – 20$. This is quite a range. For this analysis we adopt $D/d = 7$.

So when given only the PV metric we assume $\sigma = PV/4$, and $k_{max} = 7/(2D)$.

A.2 Surface vs. Reflected WFE: When a surface specification is given, we have to convert it to the total reflected wavefront error. This means that the rms will be a factor of 2 larger due to double pass in reflection, and we must also account for angle of incidence, which makes the surface error larger for anything other than 90°. So we use

$$\sigma_{refl} = 2\sigma_{surf}/\cos(\theta_i). \quad (3)$$

Note that this is an overestimate, as only one axis of the beam is subject to the $\cos(\theta_i)$ correction.

¹http://www.savvyoptics.com/files/MSF_ripple_presentationSep_26-3.pdf



MagAO-X Preliminary Design

5.1 Optics Specifications

Doc #: MagAOX-001
 Date: 2017-04-19
 Status: Rev. 0.0
 Page: 13 of 18

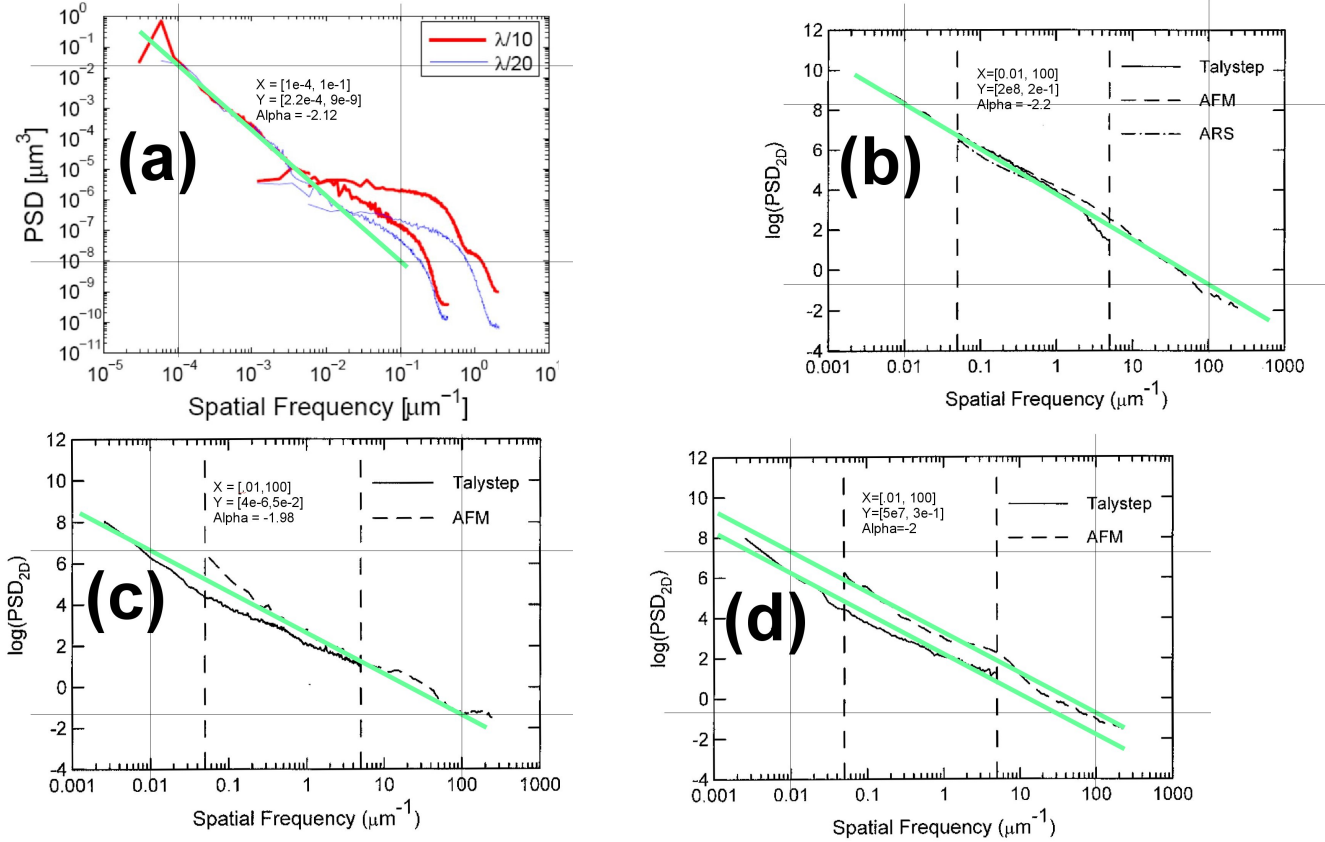


Figure 9: Measured PSDs of Flats. (a) is for 25 mm Al coated BK7 with $\lambda/10$ and $\lambda/20$ P-V from Alcock et al. (2010). (b)-(d) are from Duparré et al. (2002). (b) is a polished fused-silica flat, (c) is a polished fused-silica flat, and (d) is polished Zerodur 665. Based on these results we adopt $\alpha = 2.0$ for flats.

A.3 PSD Index: The value of α for a selection of flats was determined by “fit-by-eye” to PSDs presented in Alcock et al. (2010) and Duparré et al. (2002). The fits are illustrated in Figure 9. We adopt $\alpha = 2$ based on these results.

PSDs for aspheric optics are difficult to find in the literature. The one example located so far is by Tinker & Xin (2013). Examples for 2 optics are shown in Figure 10. These results imply $\alpha \approx 1.6$ for OAPs. In a report provided by a vendor for a single optic, they found $\alpha = 1.55$ by fitting PSD data. We will use 1.55 for all OAPs.

A.4 Surface Roughness: According to ISO-10110-8, the surface roughness is specified over length scales of 85 μm to 2.5 μm. Based on the plots from Tinker & Xin (2013) shown in Figure 10 we will assume the PSD is white in this range. That is

$$\mathcal{P}_{sr} = \beta_{sr} \quad (4)$$

with β_{sr} constant. The normalization for the PSD in this range is

$$\beta_{sr} = \frac{\sigma_{sr}^2}{\pi(k_{max}^2 - k_{min}^2)} \quad (5)$$



MagAO-X Preliminary Design

5.1 Optics Specifications

Doc #: MagAOX-001
 Date: 2017-04-19
 Status:
 Page:

Rev. 0.0
 14 of 18

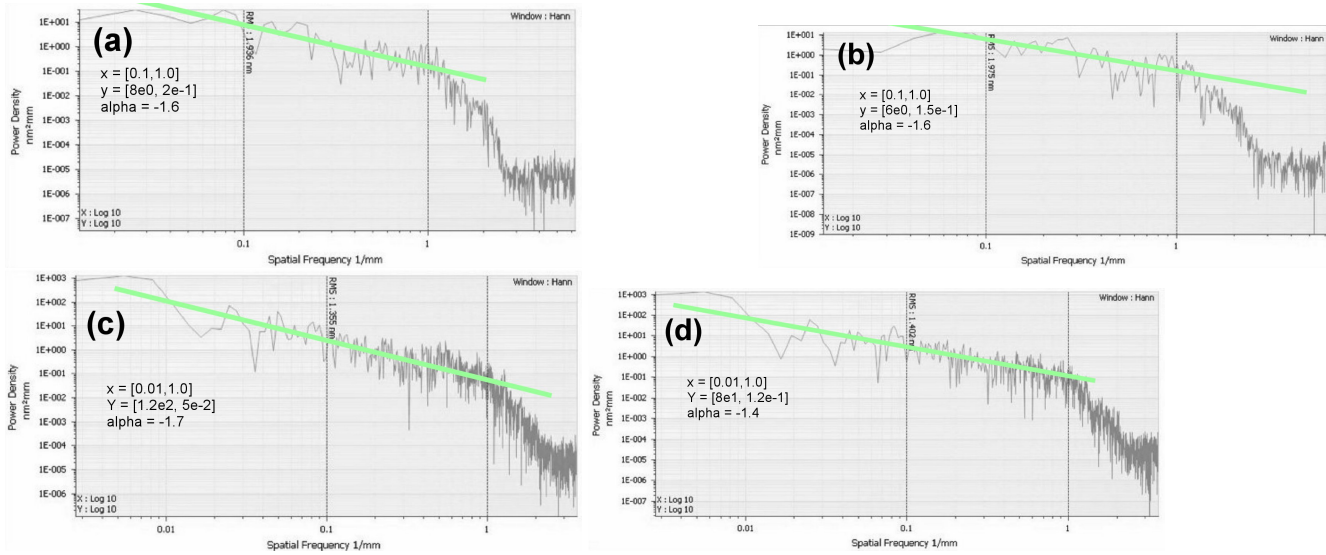


Figure 10: PSDs of manufactured SiC OAPs from Tinker & Xin (2013). (a) and (b) are cuts from the PSD of 58 mm f/1.4 OAP. (c) and (d) are cuts from a 150 mm f/1.7 OAP. The green lines show a rough “fit-by-eye” to the data.

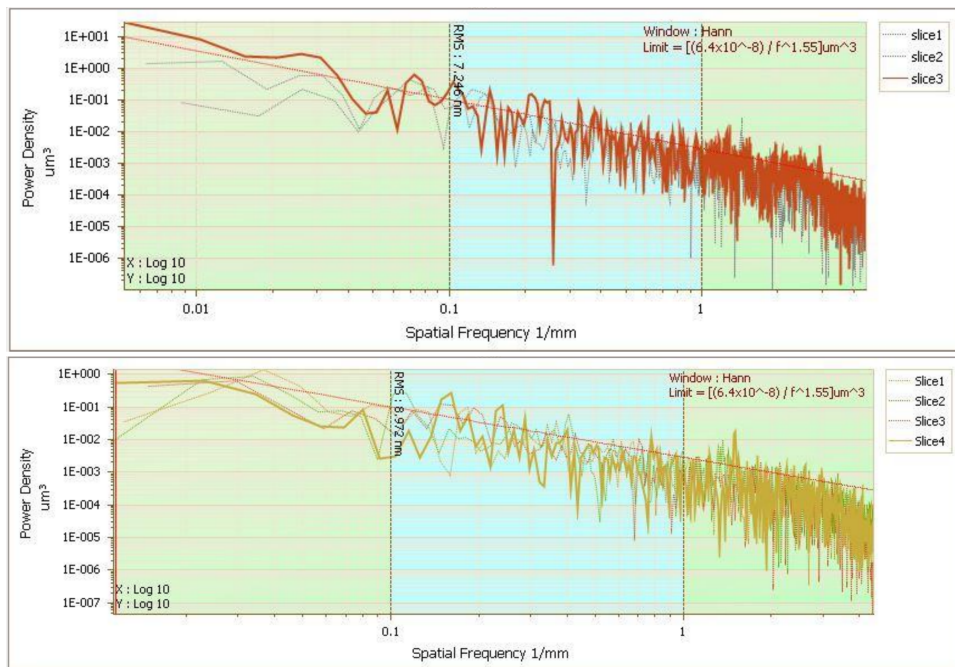


Figure 11

	MagAO-X Preliminary Design 5.1 Optics Specifications	Doc #: MagAOX-001 Date: 2017-04-19 Status: Rev. 0.0 Page: 15 of 18
---	---	---

where σ_{sr} is the surface roughness RMS, $k_{max} = 1/2.5 \mu\text{m}$, and $k_{min} = 1/85 \mu\text{m}$.

A.5 Inner Scale: Note the fall-off in the PSDs at higher spatial frequencies. In Alcock et al. (2010) it is claimed that these are due to instrument and measurement artifacts. However, the roll-off in the PSD evident in the OAP results seems to be real. This is confirmed by considering the surface roughness of these optics as we just did, since the simple power-law can not extend to infinitely high spatial frequencies and still produce the surface roughness. As is evident in Figure 10 there must be a roll-off in order to meet the surface roughness specification. This roll-off evidently has the form of an inner-scale, which can be modeled with a PSD of the form

$$\mathcal{P}(\vec{k}) = \frac{\beta}{|\vec{k}|^\alpha} e^{-(kl_0)^2} \quad (6)$$

where l_0 is the inner scale. This is illustrated in Figure 12. For the OAPs shown in 10 we estimate $l_0 \sim 0.3$. The PSDs for flats are measured at much higher spatial frequencies and do not show the same behavior, so we do not apply an inner scale to the flats.

A.6 Outer Scale: There is also a flattening at low spatial frequencies in some of the PSDs, pointing to an outer scale effect. We model this in the usual way with parameter L_0 . $L_0 = 15 \text{ mm}$ gives a reasonable match to typical OAP PSDs.

A.7 Complete PSD: Taking all of the above into account we have the final complete PSD

$$\mathcal{P}(\vec{k}) = \frac{\beta}{\left((1/L_0)^2 + |\vec{k}|^2\right)^{\alpha/2}} e^{-(|\vec{k}|l_0)^2} + \beta_{sr}. \quad (7)$$

A.8 Projections: The above characteristics apply to the entire CA. In general, the beam will be smaller than this, and be of different size on each optic in the instrument. To compensate, we project each PSD back to the primary mirror. To start with, the variance on the entire optic is

$$\sigma_{CA} = \beta_{CA} \int_{1/D_{CA}}^{k_{max}} \frac{1}{k^\alpha} k dk d\phi$$

and across the beam we have

$$\sigma_{beam} = \beta_{CA} \int_{1/D_{beam}}^{1/2d} \frac{1}{k^\alpha} k dk d\phi.$$

Now we assert that

$$\sigma_{pri} = \sigma_{beam}$$

and that

$$\frac{D}{d} = n = \text{constant}$$

for both the beam and the primary mirror. We then have

$$\beta_{pri} = \left(\frac{D_{pri}}{D_{beam}} \right)^{-\alpha+2} \beta_{CA} \quad (8)$$

for normalizing the PSD projected onto the primary mirror.

Both L_0 and l_0 scale linearly as D_{pri}/D_{CA} .

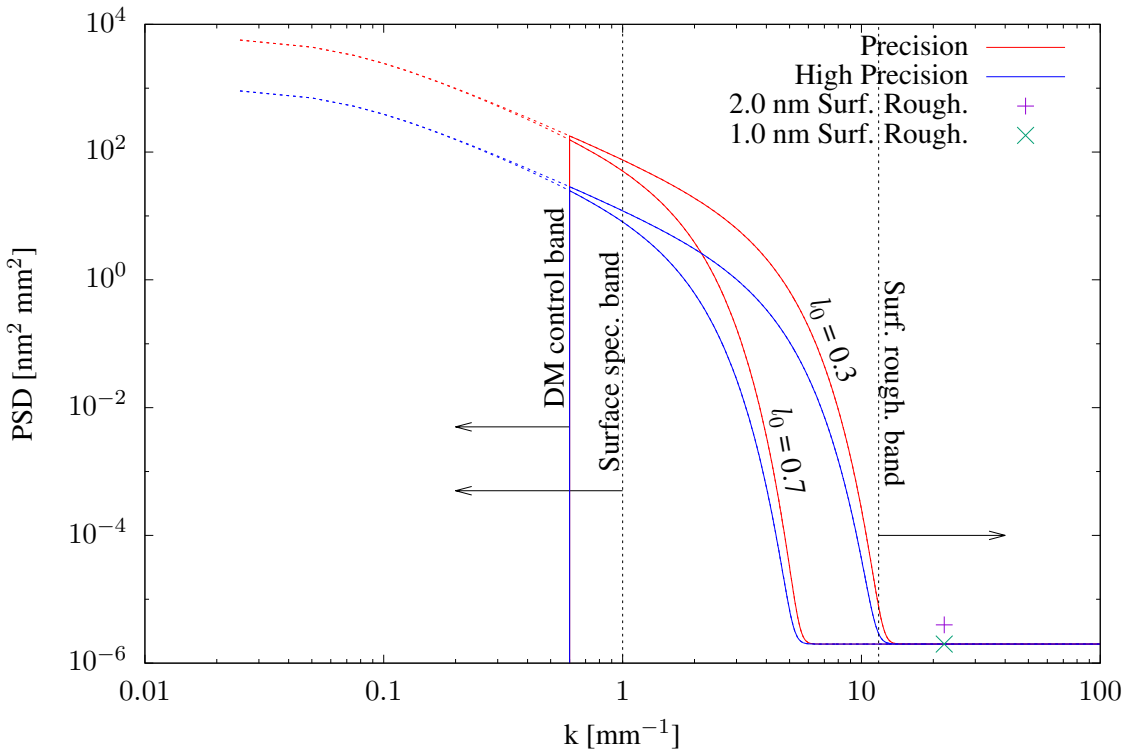


Figure 12: The complete PSD as modeled by Equation 7. Here we show PSDs for an OAP vendor's specifications, with $\alpha = 1.55$, $L_0 = 15$ mm, two choices for l_0 , and 1 nm surface roughness. Various spatial frequency bands of interest are noted.

B Clay M1

Buddy Martin of SOML provided the post-polishing measurements of the surface. The data file was processed using the C code provided by him. The header of the file contained

```
! Diffraction International conversion from Durango to Code V
! ACQ S/N: 0003-992161670
! Part #:
! Serial #:
! Surface:
! Data: 1:1]
! Subtractions: PST TLT PWR AST CMA SA3 MOR
! ROI is pixels X=11 thru X=243, Y=17 thru Y=249
```

GRD 233 233 WFR WVL 0.632820 SSZ 65536 NDA 32767

The short data values were scaled by the indicated value to be in nm of surface height in single precision. The



following plots show the results of a PSD analysis. Figure 1 shows the raw map as extracted from the data file.

Figure 13 shows the 2D PSD of the masked surface. An annular Hann window was applied, and the PSD was renormalized to have total variance corresponding to 12.52 nm rms.

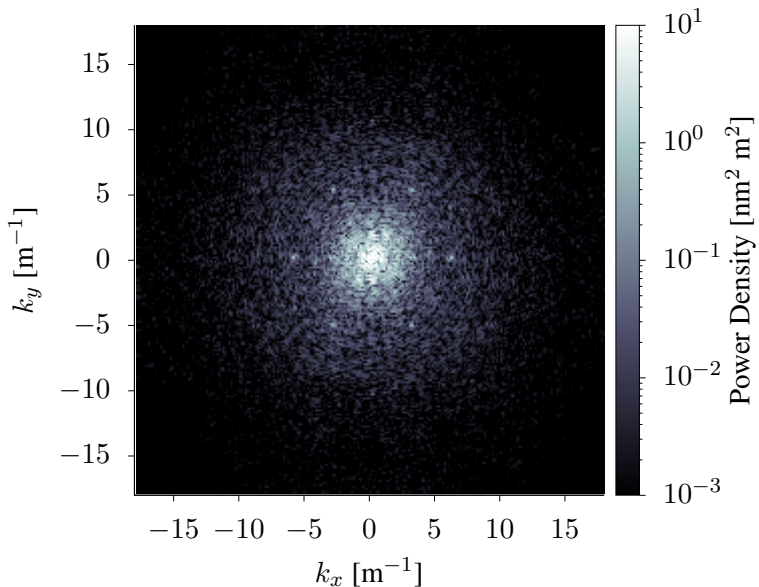


Figure 13: PSD of M1 surface.

Figure 14 shows the PSF of an image formed by using the masked surface as a pupil plane phase aberration in reflection (multiplied by 2) at 656 nm (H α).

Figure 15 shows the image formed assuming an ideal coronagraph.

References

- Alcock, S. G., Ludbrook, G. D., Owen, T., & Dockree, R. 2010, in Proc. SPIE, Vol. 7801, Advances in Metrology for X-Ray and EUV Optics III, 780108
- Duparré, A., Ferre-Borrull, J., Gleich, S., et al. 2002, Applied Optics, 41, 154
- Evans, C. J. 2009, Optical Engineering, 48, 043605
- Noll, R. J. 1976, Journal of the Optical Society of America (1917-1983), 66, 207
- Schwartz, K. 2010, Master's thesis, The University of Arizona, Tucson, AZ
- Tinker, F., & Xin, K. 2013, in Proc. SPIE, Vol. 8837, Material Technologies and Applications to Optics, Structures, Components, and Sub-Systems, 88370M

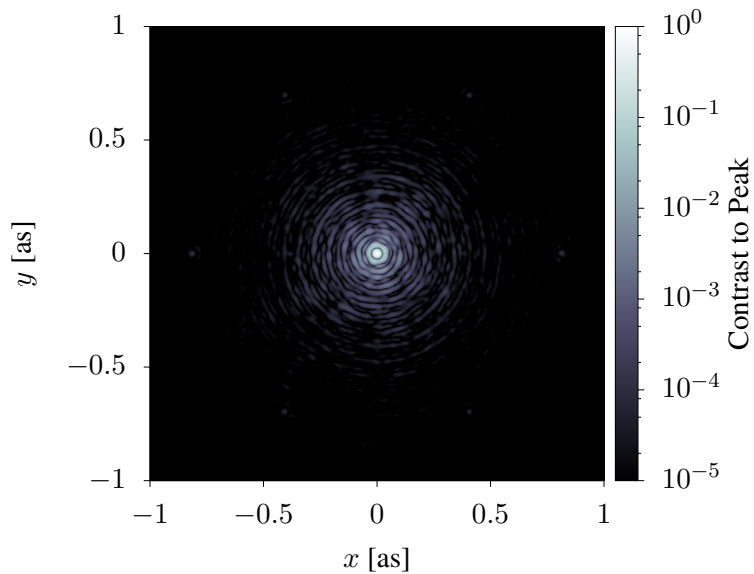


Figure 14: PSF of M1 at H α .

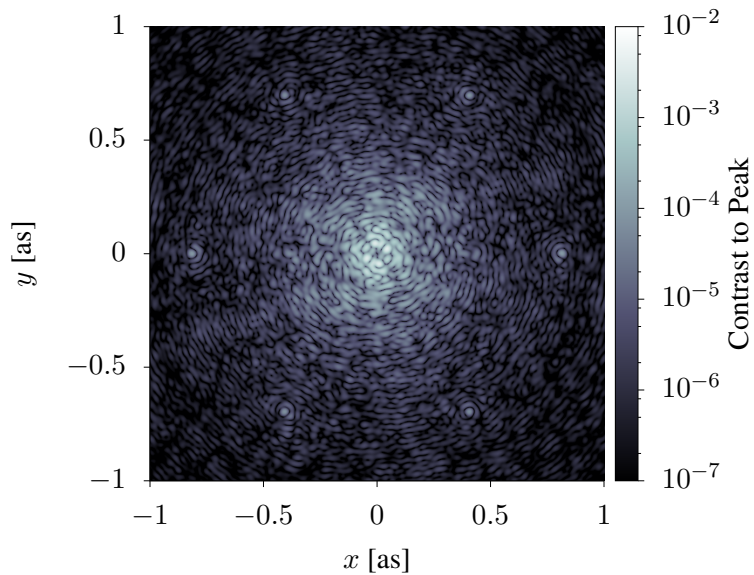


Figure 15: PSF of M1 at H α with ideal coronagraph. The 6 spots are due to print-through of the hexagonal honeycomb structure, and are observed in MagAO+VisAO diffraction-limited images.